Proceedings of the 17th World Congress
The International Federation of Automatic Control
Seoul, Korea, July 6-11, 2008

Discretized PID Control and Robust Stabilization for Continuous Plants

Yoshifumi Okuyama *

* *Humanitech Laboratory, Co., Ltd. & Tottori University(Emeritus), Japan*
(Tel: +81-88-625-2545; e-mail: oku@humanitech-lab.jp).

Abstract: This paper describes discrete-time and discrete-value (discretized/quantized) PID control and robust stabilization for continuous plants. Although all control systems are currently realized using discretized signals, the analysis and design of such nonlinear discrete-time control systems has not been elucidated. In this paper, the robust stability analysis of discrete-time and discrete-value (digital) control systems that accompany discretizing units at the input and output sides of a nonlinear element is performed in the frequency domain, and a method for achieving PID control and robust stabilization for nonlinear discretized systems on a grid pattern in the time and control variables space is presented. In the design procedure, a modified Nichols diagram and parameter specifications are applied. Numerical examples are provided to verify the validity of the designing method.

1. INTRODUCTION

At present, almost all feedback control systems are realized using discretized (discrete-time and discrete-value, i.e., digital) signals. However, the analysis and design of discretized/quantized control systems have not been completely elucidated. The first attempt to elucidate the problem was described in a paper by Kalman [1956]. Since then, many researchers have studied this problem, particularly the aspect of understanding and mitigating the quantization effects in quantized feedback control (Curry [1970], Delchamps [1990], Elia and Mitter [2001], Fu [2003]). However, few results for the stability analysis of the nonlinear discrete-time feedback system have been obtained (Willems [1971], Desoer and Vidyasagar [1975], Harris and Valenca [1983]).

This paper describes the robust stability analysis of discrete-time and discrete-value control systems and presents a method for designing (stabilizing) PID control for nonlinear discretized systems. The PID control scheme has been widely used in practice and theory irrespective of whether it is continuous or discrete in time (Datta et al. [2000], Takemori and Okuyama [2000]), since it is a basic feedback control technique.

In the previous study (Okuyama [2006]), a robust stability condition for nonlinear discretized control systems that accompany discretizing units (quantizers) at equal spaces was examined in a frequency domain. It was assumed that the discretization is executed at the input and output sides of a nonlinear actuator and that the sampling period is chosen such that it is suitable for discretization in the space. This paper presents a designing problem for discretized control systems on a grid pattern in the time and controller variables space. In this study, the concept of modified Nyquist and Nichols diagrams for nonlinear control systems explained in Okuyama et al. [1999, 2002a] is applied to the design procedure in the frequency domain.

2. DISCRETIZED CONTROL SYSTEM

The discretized control system in question is represented by a sampled-data (discrete-time) feedback system with two samplers, S_1 and S_2, as shown in Fig. 1. Here, $\mathcal{D}$ and $\mathcal{H}$ denote the

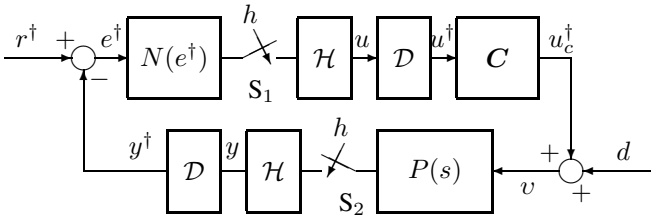

Fig. 1. Nolinear sampled-data PID control system.

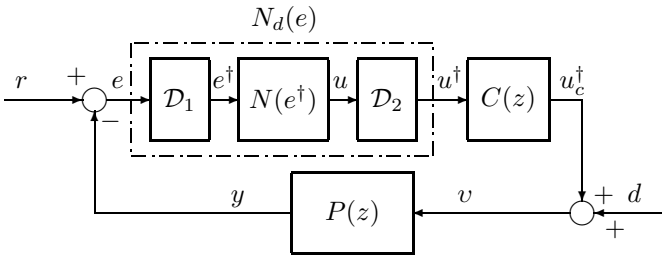

Fig. 2. Discretized nonlinear PID control system.

unit for the discretization and the zero-order holding, respectively, which are usually performed in the A/D (D/A) conversion. Moreover, $N(\cdot)$, $\boldsymbol{C}$, and $P(s)$ are a nonlinear continuos element, digital controller (compensator) based on the PID control scheme, and linear continuous plant (physical system to be controlled), respectively. Here, the linear/nonlinear characteristic of continuous element $N(\cdot)$ is not very important because the discretization is a (stepwise) nonlinear characteristic. (Even if it is a linear characteristic, the following nonlinear analysis is needed.)

When the two samplers operate synchronously with a sampling period h, the nonlinear sampled-data control system can be transformed into a discrete-time control system as shown in Fig. 2. Here, $P(z)$ is the z-transform of $P(s)$ together with the zero-order hold, $C(z)$ is the z-transform of the digital PID controller $\boldsymbol{C}$, and $\mathcal{D}_1$ and $\mathcal{D}_2$ are the discretization units at the input and output sides of the nonlinear continuous element (actuator/sensor), respectively. The relationship between e and

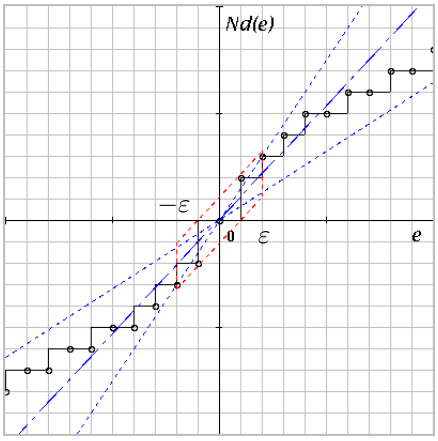

Fig. 3. Discretized nonlinear characteristics on a grid pattern.

$u^\dagger = N_d(e)$ becomes a stepwise nonlinear characteristic on a grid pattern as shown in Fig. 3. In this study, a round-down discretization, which is usually executed on a computer, is applied. Therefore, the relationship between $e^\dagger$ and $u^\dagger$ is indicated by small circles on the stepwise nonlinear characteristic.

In Figs. 1 and 2, the symbols e, u, $\cdots$ indicate the sequences $e(k)$, $u(k)$, $\cdots$, $(k = 0, 1, 2, \cdots)$ in discrete time, but for continuous value. Each symbol $e^\dagger$, $u^\dagger$, $\cdots$ indicates discrete value that can be assigned to an integer number, e.g.,

$$e^\dagger \in \{\cdots, -3\gamma, -2\gamma, -\gamma, 0,\ \gamma,\ 2\gamma,\ 3\gamma, \cdots\},$$
$$u^\dagger \in \{\cdots, -3\gamma, -2\gamma, -\gamma, 0,\ \gamma,\ 2\gamma,\ 3\gamma, \cdots\},$$

where γ is the resolution of each variable. In the above expression, it is assumed that the input and output signals of the nonlinear characteristic have the same resolution in the discretization. Here, $e^\dagger$, $u^\dagger$, $\cdots$ also represent the sequences $e^\dagger(k)$, $u^\dagger(k)$, $\cdots$, respectively. Without loss of generality, hereafter, we assume that $\gamma = 1.0$.

On the other hand, the time variable t can be defined as follows:

$$t \in \{0, h,\ 2h,\ 3h, \cdots\},$$

where h is the sampling period. In other words, the integer time sequence can be defined as follows:

$$k \in Z_+, \quad Z_+ = \{0, 1, 2, 3, \cdots\}.$$

That is, the variables $e^\dagger(k)$ and $u^\dagger(k)$ are defined on a grid pattern that is composed of integers in the time and controller variables space.

In this study, the stepwise nonlinear characteristic of the controller, as shown in Fig. 3, can be represented by the following equation:

$$N_d(e) = Ke + g(e), \quad 0 < K < \infty. \tag{1}$$

It is partitioned into the following two sections:

$$|g(e)| \le \bar{g} < \infty, \tag{2}$$

for $|e| < \varepsilon$ and

$$|g(e)| \le \beta\,|e|, \quad 0 \le \beta < \infty, \tag{3}$$

for $|e| \ge \varepsilon$. Equation (2) represents a bounded nonlinear characteristic that exists in a finite region. On the other hand, equation (3) represents a sectorial nonlinearity for which the equivalent linear gain exists in a limited range. It can also be expressed as follows:

$$0 \le g(e)e \le \beta e^2. \tag{4}$$

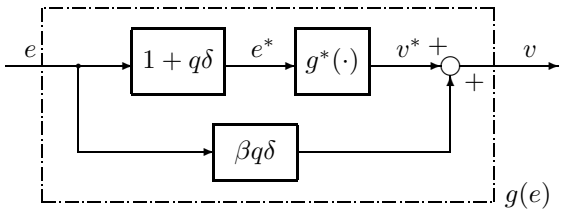

Fig. 4. Nonlinear subsystem.

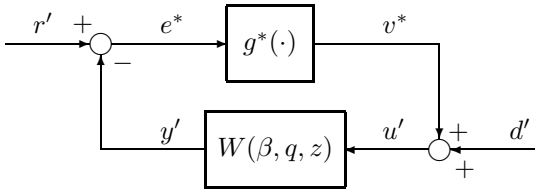

Fig. 5. Equivalent feedback system.

When considering the robust stability in a global sense, it is sufficient to consider the nonlinear term (3) for $|e| \ge \varepsilon$ because the nonlinear term (2) can be treated as a disturbance signal (Okuyama [2006]). (In this study, a fluctuation or an offset of error is assumed to be allowable in $|e| < \varepsilon$.)

3. EQUIVALENT DISCRETE-TIME SYSTEM

Based on the above consideration, the following new sequences $e_m^{*\dagger}(k)$ and $v_m^{*\dagger}(k)$ are defined as:

$$e_m^{*\dagger}(k) = e_m^\dagger(k) + q \cdot \frac{\Delta e^\dagger(k)}{h}, \tag{5}$$

$$v_m^{*\dagger}(k) = v_m^\dagger(k) - \beta q \cdot \frac{\Delta e^\dagger(k)}{h}. \tag{6}$$

where q is a non-negative number, $e_m^\dagger(k)$ and $v_m^\dagger(k)$ are neutral points of sequences $e^\dagger(k)$ and $v^\dagger(k)$,

$$e_m^\dagger(k) = \frac{e^\dagger(k) + e^\dagger(k-1)}{2}, \tag{7}$$

$$v_m^\dagger(k) = \frac{v^\dagger(k) + v^\dagger(k-1)}{2}, \tag{8}$$

and $\Delta e^\dagger(k)$ is the backward difference of $e^\dagger(k)$,

$$\Delta e^\dagger(k) = e^\dagger(k) - e^\dagger(k-1). \tag{9}$$

The relationship between equations (5) and (6) with respect to the continuous values is shown by the block diagram in Fig. 4. In this figure, δ is defined as

$$\delta(z) := \frac{2}{h} \cdot \frac{1 - z^{-1}}{1 + z^{-1}}. \tag{10}$$

Equation (10) corresponds to the bilinear transformation between z and δ. Thus, the loop transfer function from v^* to e^* can be given by $W(\beta, q, z)$, as shown in Fig. 5, where

$$W(\beta, q, z) = \frac{(1 + q\delta(z))P(z)C(z)}{1 + (K + \beta q\delta(z))P(z)C(z)}, \tag{11}$$

and r' and d' are transformed exogenous inputs. Here, the variables such as v^*, u' and y' written in Fig. 5 indicate the z-transformed ones.

In this paper, the following assumption is provided on the basis of the relatively fast sampling and the slow response of the

controlled system.

Assumption The absolute value of the backward difference of sequence $e(k)$ does not exceed γ, i.e.,

$$|\Delta e(k)| = |e(k) - e(k-1)| \leq \gamma. \tag{12}$$

If condition (12) is satisfied, $\Delta e^{\dagger}(k)$ defined by (9) is exactly $\pm\gamma$ or 0 because of the discretization. That is, the absolute value of the backward difference can be given as

$$|\Delta e^{\dagger}(k)| = |e^{\dagger}(k) - e^{\dagger}(k-1)| = \gamma \text{ or } 0. \quad \square$$

The assumption stated above will be satisfied by the following examples. The phase trace of $\Delta e^{\dagger}$ is shown in the figure.

4. NORM INEQUALITIES

In this section, some lemmas with respect to an ℓ_2 norm of the sequences are presented. Here, we define a new nonlinear function

$$f(e) := g(e) + \beta\, e. \tag{13}$$

When considering the discretized output of the nonlinear characteristic, $v^{\dagger} = g(e^{\dagger})$, the following expression can be given:

$$f(e^{\dagger}(k)) = v^{\dagger}(k) + \beta e^{\dagger}(k). \tag{14}$$

From inequality (3), it can be seen that the function (14) belongs to the first and third quadrants.

When considering the equivalent linear characteristic, the following inequality can be defined:

$$0 \leq \psi(k) := \frac{f(e^{\dagger}(k))}{e^{\dagger}(k)} \leq 2\beta. \tag{15}$$

When this type of nonlinearity $\psi(k)$ is used, inequality (3) can be expressed as

$$v^{\dagger}(k) = g(e^{\dagger}(k)) = (\psi(k) - \beta)e^{\dagger}(k). \tag{16}$$

For the neutral points of $e^{\dagger}(k)$ and $v^{\dagger}(k)$, the following expression is given from (14):

$$\frac{1}{2}(f(e^{\dagger}(k)) + f(e^{\dagger}(k-1))) = v_m^{\dagger}(k) + \beta e_m^{\dagger}(k). \tag{17}$$

Moreover, equation (16) is rewritten as

$$v_m^{\dagger}(k) = (\psi(k) - \beta)e_m^{\dagger}(k).$$

Since $|e_m^{\dagger}(k)| \leq |e_m(k)|$, the following inequality is satisfied when a round-down discretization is executed:

$$|v_m^{\dagger}(k)| \leq \beta|e_m^{\dagger}(k)| \leq \beta|e_m(k)|. \tag{18}$$

Based on the above premise, the following norm conditions are examined (Okuyama [2006]).

Lemma 1. The following inequality holds for a positive integer p:

$$\|v_m^{\dagger}(k)\|_{2,p} \leq \beta\|e_m^{\dagger}(k)\|_{2,p} \leq \beta\|e_m(k)\|_{2,p}. \tag{19}$$

Here, $\|\cdot\|_{2,p}$ denotes the Euclidean norm, which can be defined by

$$\|x(k)\|_{2,p} := \left(\sum_{k=1}^{p} x^2(k)\right)^{1/2}.$$

Proof. The proof is clear from inequality (18). □

Lemma 2. If the following inequality is satisfied with respect to the inner product of the neutral points of (14) and the backward difference (9):

$$\langle\, v_m^{\dagger}(k) + \beta e_m^{\dagger}(k), \Delta e^{\dagger}(k)\,\rangle_p \geq 0, \tag{20}$$

the following inequality can be obtained:

$$\|v_m^{*\dagger}(k)\|_{2,p} \leq \beta\|e_m^{*\dagger}(k)\|_{2,p} \tag{21}$$

for any $q \geq 0$. Here, $\langle\cdot,\cdot\rangle_p$ denotes the inner product, which is defined as

$$\langle\, x_1(k), x_2(k)\,\rangle_p = \sum_{k=1}^{p} x_1(k)x_2(k).$$

Proof. The following equation is obtained from (5) and (6):

$$\begin{aligned}
&\beta^2\|e_m^{*\dagger}(k)\|_{2,p}^2 - \|v_m^{*\dagger}(k)\|_{2,p}^2 \\
&\quad = \beta^2\|e_m^{\dagger}(k)\|_{2,p}^2 - \|v_m^{\dagger}(k)\|_{2,p}^2 \\
&\qquad + \frac{2\beta q}{h} \cdot \langle v_m^{\dagger}(k) + \beta e_m^{\dagger}(k), \Delta e^{\dagger}(k)\rangle_p.
\end{aligned} \tag{22}$$

Thus, (21) is satisfied by using the left inequality of (19).

Moreover, as for the input of $g^*(\cdot)$, the following inequality can be obtained from (22) and the right inequality of (19):

$$\|v_m^{*\dagger}(k)\|_{2,p} \leq \beta\|e_m^{*}(k)\|_{2,p}, \tag{23}$$

when inequality (20) is satisfied. □

The left side of inequality (20) can be expressed as a sum of trapezoidal areas.

Lemma 3. For any step p, the following equation is satisfied:

$$\begin{aligned}
\sigma(p) &:= \langle\, v_m^{\dagger}(k) + \beta e_m^{\dagger}(k), \Delta e^{\dagger}(k)\,\rangle_p \\
&= \frac{1}{2}\sum_{k=1}^{p}(f(e^{\dagger}(k)) + f(e^{\dagger}(k-1)))\Delta e^{\dagger}(k).
\end{aligned} \tag{24}$$

Proof. The proof is clear from (17). □

In general, the sum of trapezoidal areas holds the following property.

Lemma 4. If inequality (12) is satisfied with respect to the discretization of the control system, the sum of trapezoidal areas becomes non-negative for any p, that is,

$$\sigma(p) \geq 0. \tag{25}$$

Proof. Since $f(e^{\dagger}(k))$ belongs to the first and third quadrants, the area of each trapezoid

$$\tau(k) := \frac{1}{2}(f(e^{\dagger}(k)) + f(e^{\dagger}(k-1)))\Delta e^{\dagger}(k) \tag{26}$$

is non-negative when $e(k)$ increases (decreases) in the first (third) quadrant. On the other hand, the trapezoidal area $\tau(k)$ is non-positive when The sum of trapezoidal area is given from (24) as:

$$\sigma(p) = \sum_{k=1}^{p} \tau(k). \tag{27}$$

Therefore, the following result is derived based on the above.

The sum of trapezoidal areas becomes non-negative, $\sigma(p) \geq 0$, regardless of whether $e(k)$ (and $e^{\dagger}$(k)) increases or decreases. Since the discretized output traces the same points on the stepwise nonlinear characteristic, the sum of trapezoidal areas is canceled when $e(k)$ (and $e^{\dagger}(k)$ decreases (increases) from a certain point $(e^{\dagger}(k), f(e^{\dagger}(k)))$ in the first (third) quadrant. (Here, without loss of generality, the response of discretized point $(e^{\dagger}(k), f(e^{\dagger}(k)))$ is assumed to commence at the origin.) Thus, the proof is concluded. □

5. ROBUST STABILITY IN A GLOBAL SENSE

By applying a small gain theorem to the loop transfer characteristic (11), the following robust stability condition of the discretized nonlinear control system can be derived.

Theorem 5. If there exists a $q \geq 0$ in which the sector parameter β with respect to nonlinear term $g(\cdot)$ satisfies the following inequality, the discrete-time control system with sector nonlinearity (3) is robust stable in an ℓ_2 sense:

$$\beta < \beta_0 = K\eta(q_0, \omega_0) = \max_q \min_\omega K\eta(q, \omega), \qquad (28)$$

when the linearized system with nominal gain K is stable. (That is, the allowable sector can be given as $[0, \beta_0]$ from (28).) Here, the η-function is written as follows:

$$\eta(q,\omega) := \frac{-q\Omega V + \sqrt{q^2\Omega^2V^2 + (U^2+V^2)\{(1+U)^2+V^2\}}}{U^2+V^2}, \quad \forall\omega \in [0, \omega_c]. \qquad (29)$$

Moreover, $\Omega(\omega)$ is the distorted frequency of angular frequency ω and is given by

$$\delta(\mathrm{e}^{j\omega h}) = j\Omega(\omega) = j\frac{2}{h}\tan\left(\frac{\omega h}{2}\right), \quad j = \sqrt{-1} \qquad (30)$$

and ω_c is a cut-off frequency. In addition, $U(\omega)$ and $V(\omega)$ are the real and the imaginary parts of $KP(\mathrm{e}^{j\omega h})C(\mathrm{e}^{j\omega h})$, respectively.

By using the polar coordinates, the following expression can be given:

$$KP(\mathrm{e}^{j\omega h})C(\mathrm{e}^{j\omega h}) = \rho(\omega)\mathrm{e}^{j\theta(\omega)}. \qquad (31)$$

In this case, equality (29) can be expressed as follows:

$$\eta(q,\omega) := \frac{-q\Omega\sin\theta + \sqrt{q^2\Omega^2\sin^2\theta + \rho^2 + 2\rho\cos\theta + 1}}{\rho}, \quad \forall\omega \in [0, \omega_c]. \qquad (32)$$

Proof. Based on the loop characteristic in Fig. 5, the following inequality can be given with respect to $z = \mathrm{e}^{j\omega h}$:

$$\|e_m^*(z)\|_{2,p} \leq c_1\|r_m'(z)\|_{2,p} + c_2\|d_m'(z)\|_{2,p} + \sup_{z=1}|W(\beta,q,z)| \cdot \|w_m^{*\dagger}(z)\|_{2,p}. \qquad (33)$$

Here, $r_m'(z)$ and $d_m'(z)$ denote the z-transformation for the neutral points of sequences $r'(k)$ and $d'(k)$, respectively. Moreover, c_1 and c_2 are positive constants.

By applying inequality (23), the following expression is obtained:

$$\left(1 - \beta\cdot\sup_{z=1}|W(\beta,q,z)|\right)\|e_m^*(z)\|_{2,p} \leq c_1\|r_m'(z)\|_{2,p} + c_2\|d_m'(z)\|_{2,p}. \qquad (34)$$

Therefore, if the following inequality (i.e., the small gain theorem with respect to ℓ_2 gains) is valid,

$$|W(\beta,q,\mathrm{e}^{j\omega h})| = \left|\frac{(1+jq\Omega(\omega))P(\mathrm{e}^{j\omega h})C(\mathrm{e}^{j\omega h})}{1+(K+j\beta q\Omega(\omega))P(\mathrm{e}^{j\omega h})C(\mathrm{e}^{j\omega h})}\right| = \left|\frac{(1+jq\Omega(\omega))\rho(\omega)\mathrm{e}^{j\theta(\omega)}}{K+(K+j\beta q\Omega(\omega))\rho(\omega)\mathrm{e}^{j\theta(\omega)}}\right| < \frac{1}{\beta}. \qquad (35)$$

the sequences $e_m^*(k)$, $e_m(k)$, $e(k)$ and $y(k)$ in the feedback system are restricted in finite values when exogenous inputs $r(k)$, $d(k)$ are finite and $p \to \infty$. (The definition of ℓ_2 stable for discrete-time systems was given in Okuyama et al. [1999, 2002a].)

From the square of both sides of inequality (35), inequality (28) is given. □

6. MODIFIED NICHOLS DIAGRAM

In the previous papers (Okuyama et al. [1999, 2002a]), the inverse function was used instead of the η-function, i.e., $\xi(q,\omega) = \dfrac{1}{\eta(q,\omega)}$. Using the notation, inequality (28) can be rewritten as follows:

$$M_0 = \xi(q_0,\omega_0) = \min_q \max_\omega \xi(q,\omega) < \frac{K}{\beta}. \qquad (36)$$

When $q = 0$, the ξ-function can be expressed as:

$$\xi(0,\omega) = \frac{\rho}{\sqrt{\rho^2 + 2\rho\cos\theta + 1}} = |T(\mathrm{e}^{j\omega h})|, \qquad (37)$$

where $T(z)$ is the complementary sensitivity function for the discrete-time system.

It is evident that the following curve on the gain-phase plane,

$$\xi(0,\omega) = M, \quad (M : \text{const.}) \qquad (38)$$

corresponds to the contour of the constant M in the Nichols diagram. In this study, since an arbitrary non-negative number q is considered, the ξ-function that corresponds to (37) and (38) is given as follows:

$$\frac{\rho}{-q\Omega\sin\theta + \sqrt{q^2\Omega^2\sin^2\theta + \rho^2 + 2\rho\cos\theta + 1}} = M. \qquad (39)$$

From this expression, the following quadratic equation can be obtained:

$$(M^2-1)\rho^2 + 2\rho M(M\cos\theta - q\Omega\sin\theta) + M^2 = 0. \qquad (40)$$

The solution of this equation is expressed as follows:

$$\rho = -\frac{M}{M^2-1}(M\cos\theta - q\Omega\sin\theta) \pm \frac{M}{M^2-1}\sqrt{(M\cos\theta - q\Omega\sin\theta)^2 - (M^2-1)}. \qquad (41)$$

The modified contour in the gain-phase plane (θ, ρ) is drawn based on the equation given in (41). Although the distorted frequency Ω is a function of ω, the term $q\Omega = c_q \geq 0$ is assumed to be a constant parameter. This assumption for M contours was also discussed in Okuyama et al. [2002a]. Figure 6 shows an example of the modified Nichols diagram for $c_q \geq 0$ and $M = 1.4$. Here, GP_1 is a gain-phase curve that touches an M contour at the peak value ($M_p = \xi(0,\omega_p) = 1.4$). On the other hand, GP_2 is a gain-phase curve that crosses the $\theta = -180^\circ$ line and all the M contours at the gain crossover point G_c. That is, the gain margin g_M becomes equal to

$$-20\log_{10}\frac{M}{M+1} = 4.68\ [\mathrm{dB}]. \qquad (42)$$

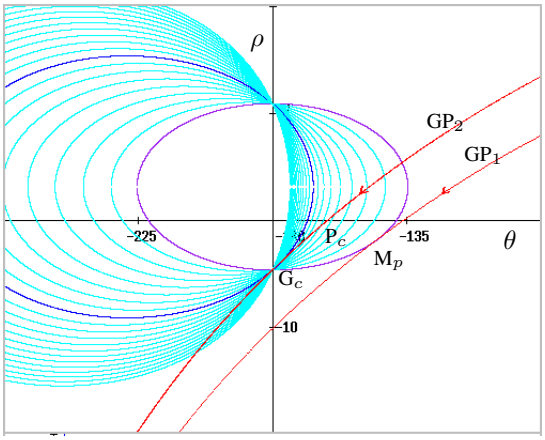

Fig. 6. Modified Nichols diagram and gain-phase curves ($M = 1.4$, $c_q = 0.0, \cdots, 4.0$).

The latter case corresponds to the discrete-time system in which Aizerman's conjecture is valid (Okuyama et al. [1998]). At the continuous saddle point G_c, the following equation is satisfied:

$$\left(\frac{\partial \xi(q,\omega)}{\partial q}\right)_{q=q_0,\omega=\omega_0} = 0. \tag{43}$$

Evidently, the phase margin p_M is obtained from the phase crossover point P_c (e.g., Brown and Campbell [1948]).

7. CONTROLLER DESIGN

The PID controller $\boldsymbol{C}$ applied in this study is given by the following algorithm:

$$u_c(k) = K_p u^\dagger(k) + C_i \sum_{j=0}^{k} u^\dagger(j) + C_d \Delta u^\dagger(k), \tag{44}$$

where $\Delta u^\dagger(k) = u^\dagger(k) - u^\dagger(k-1)$ is the backward difference of integers, and each coefficient is defined as

$$K_p,\ C_i,\ C_d \in Z_+, \quad Z_+ = \{0, 1, 2, 3 \cdots\}.$$

Here, K_p, C_i, and C_d correspond to K_p, $K_p h/T_I$, and $K_p T_D/h$ in the following (discrete-time z-transform expression) PID algorithm:

$$C(z) = K_p \left(1 + \frac{h}{T_I(1-z^{-1})} + \frac{T_D}{h}(1-z^{-1})\right). \tag{45}$$

We use algorithm (44) without division because $u^\dagger$, u_c, and coefficients K_p, C_i, C_d are integers.

Using the z-transform expression, equation (44) can be written as:

$$\begin{aligned} u_c(z) &= C(z)u(z) \\ &= \left(K_p + C_i(1 + z^{-1} + z^{-2} + \cdots) + C_d(1 - z^{-1})\right) u(z). \end{aligned}$$

In the closed form, controller $C(z)$ can be given as

$$\begin{aligned} C(z) &= K_p + C_i \cdot \frac{1}{1-z^{-1}} + C_d(1-z^{-1}) \\ &= \frac{K_p(1-z^{-1}) + C_i + C_d(1-z^{-1})^2}{1-z^{-1}} \end{aligned} \tag{46}$$

for discrete-time systems. When equations (45) and (46) are compared, C_i and C_d become equal to $K_p h/T_I$ and $K_p T_D/h$, respectively.

Table 1. PID parameters for Example-1 (g_M: gain margins, p_M: phase margins, β_0: allowable sectors, M_p: peak values)

	K_p	C_i	C_d	β_0	g_M[dB]	p_M[deg]	M_p
(i)	200	0	0	0.71	4.6	18.2	3.4
(ii)	100	0	0	1.23	10.6	46.2	1.32
(iii)	100	2	20	1.02	8.8	30.7	1.93
(iv)	100	4	20	0.92	5.64	15.9	3.70
(v)	100	2	40	1.02	9.18	32.1	1.87
(vi)	100	4	40	0.97	6.12	16.7	3.50
(vii)	80	1	20	1.07	11.8	45.8	1.31
(viii)	60	1	20	1.06	14.0	52.3	1.15

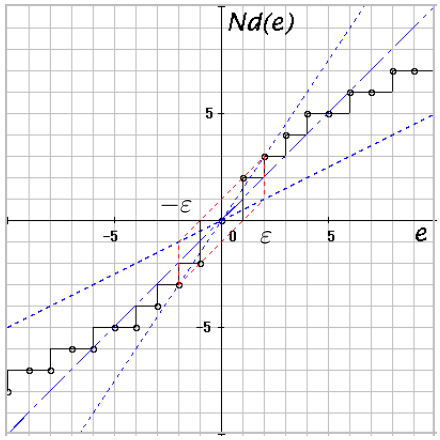

Fig. 7. Discretized nonlinear characteristics.

The design method adopted in this paper is based on the classical parameter specifications presented in the modified Nichols diagram. This method can be conveniently designed, and it is significant in a physical sense (i.e., mechanical vibration and resonance).

8. NUMERICAL EXAMPLES

[Example-1] Consider the following plant:

$$P(s) = \frac{K_1}{(s+0.02)(s+0.1)(s+0.2)}, \tag{47}$$

where $K_1 = 0.00002 = 2.0 \times 10^{-5}$. (The gain constant is defined as such a small number because the PID parameters are integers.) The discretized nonlinear characteristic (discretized sigmoid, i.e. arc tangent (Okuyama et al. [2002b]) is as shown in Fig. 7. Here, the resolution value is $\gamma = 1$ as described in section 2. For C-language expression, it can be written as

$$\begin{aligned} e^\dagger &= \gamma * (\text{double})(\text{int})(e/\gamma) \\ u &= 0.4 * e^\dagger + 3.0 * \text{atan}(0.6 * e^\dagger) \\ u^\dagger &= \gamma * (\text{double})(\text{int})(u/\gamma), \end{aligned}$$

where (int) and (double) denote the conversion into an integral number (a round-down discretization) and the reconversion into a double-precision real number, respectively. In this paper, the sampling period is chosen as a base unit $h = 1.0$.

When choosing the nominal gain $K = 1.0$ and the threshold $\varepsilon = 2.0$, the sectorial area of the stepwise nonlinear characteristic for $\varepsilon \le |e|$ can be determined as [0.5, 1.5] drawn

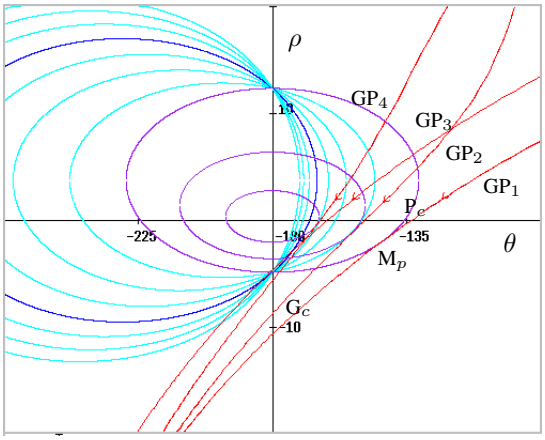

Fig. 8. Modified Nichols diagram and gain-phase curves for Example-1 ($M = 1.4$, $c_q = 0.0, \cdots, 4.0$).

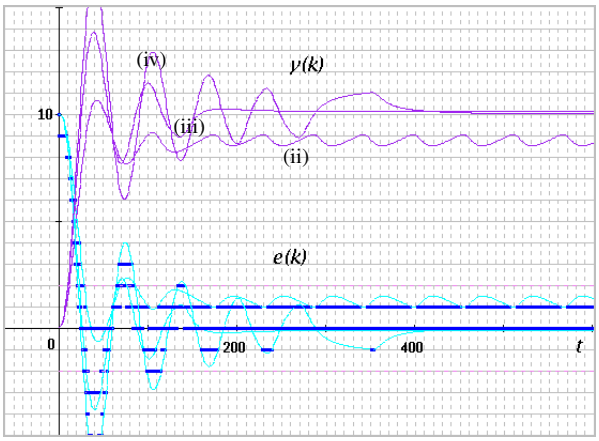

Fig. 9. Step responses for Example-1 ((ii), (iii), and (iv)).

by dotted lines in the figure. Fig. 8 shows gain-phase curves of $KP(\mathrm{e}^{j\omega h})C(\mathrm{e}^{j\omega h})$ on the modified Nichols diagram. Here, GP_1, GP_2, GP_3, and GP_4 are cases (i), (ii), (iii), and (iv), respectively. The PID parameters are specified as shown in Table 1. The gain margins g_M, the phase margin p_M and the peak value M_p can be obtained from the gain crossover points G_c, the phase crossover points P_c, and the points of contact with the M contours, respectively.

The max-min value β_0 is calculated from (28) and (29) (e.g., (i)) as follows:

$$\beta_0 = \max \eta(q, \omega_0) = \eta(q_0, \omega_0) = 0.71.$$

Thus, the allowable sector for nonlinear characteristic $g(\cdot)$ is given as [0.0, 1.71]. The stability of discretized control system (i) (and also systems (ii)-(viii)) will be guaranteed. In this example, the continuous saddle point (43) appears (i.e., Aizerman's conjecture is satisfied). The allowable sector of equivalent linear gain K_ℓ can be given as $0 < K_\ell < 1.71$.

Figures 9, 11 and 12 show time responses for the eight cases, and Figure 10 shows the phase traces of cases (ii), (iii) and (iv). As is obvious from the figure, *Assumtion* (12) is satisfied. In Fig. 9 the step response (ii) remains a sutained oscillation and an off-set. However, as for (iii) and (iv) the responses are improved by using the PID, especially integral (I: a summation

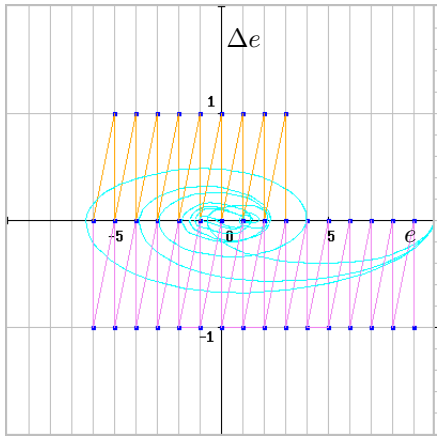

Fig. 10. Phase traces for Example-1 (cases (ii), (iii), and (iv)).

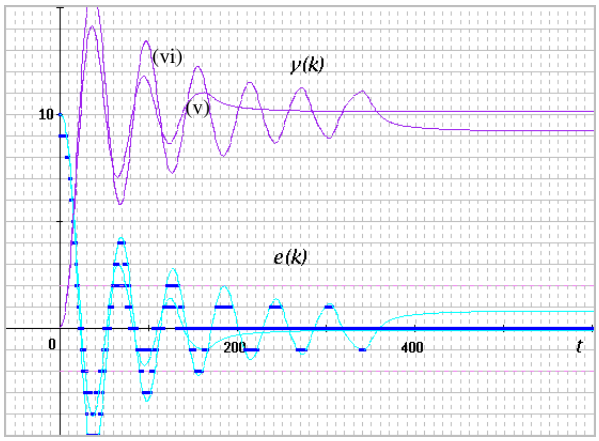

Fig. 11. Step responses for Example-1 (cases (v) and (vi)).

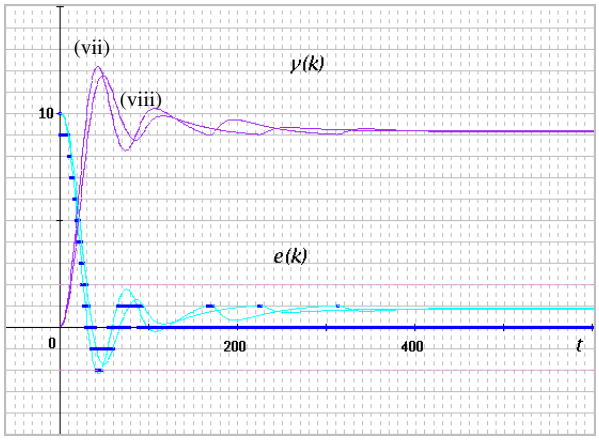

Fig. 12. Step responses for Example-1 (cases (vii) and (viii)).

in this study) algorithm.

[Example-2] Consider the following plant:

$$P(s) = \frac{K_2(s + 0.1)(-s + 0.2)}{(s + 0.01)(s + 0.02)(s + 0.5)}, \qquad (48)$$

where $K_2 = 0.0005 = 5.0 \times 10^{-4}$. The same nonlinear characteristic and the nominal gain are chosen as shown in Example-1. The modified Nichols diagram with gain-phase

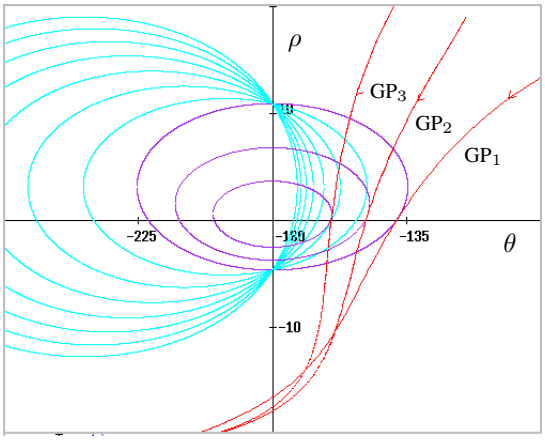

Fig. 13. Modified Nichols diagram and gain-phase curves for Example-2 ($M = 1.09$, $c_q = 0.0, \cdots, 4.0$).

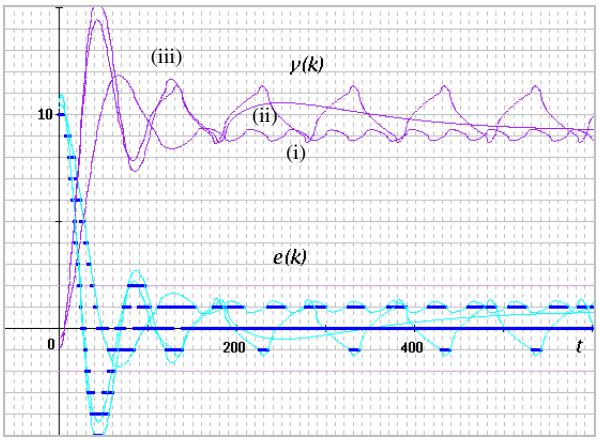

Fig. 14. Step responses for Example-2.

curves of $KP(e^{j\omega h})C(e^{j\omega h})$ is as shown in Fig. 13. Here, GP_1, GP_2 and GP_3 are cases (i), (ii), and (iii), and the PID parameters are specified as shown in Table 1. Figure 14 shows time responses for the three cases. In this example, although the allowable sector of equivalent linear gain (e.g., case (iii)) is $0 < K_\ell < 3.1$, the allowable sector for nonlinear characteristic becomes [0.0, 1.42] as shown in Table 2. Since the sectorial area of the stepwise nonlinear characteristic is [0.5, 1.5], the stability of the nonlinear control system cannot be guaranteed. The response for (iii) actually fluctuates as shown in Fig. 14. This is a counter example for Aizerman's conjecture (Okuyama et al. [1998]).

Table 2. PID parameters for Example-2 (g_M: gain margins, p_M: phase margins, β_0: allowable sectors, M_p: peak values)

	K_p	C_i	C_d	β_0	g_M [dB]	p_M [deg]	M_p
(i)	100	0	0	0.94	16.6	42.3	1.40
(ii)	100	1	100	0.61	8.8	31.3	1.85
(iii)	100	2	100	0.42	17.5	19.9	2.93

9. CONCLUSION

In this paper, we have described the discrete-time discrete-value PID control and robust stabilization for continuous plants. A robust stability condition for nonlinear discretized feedback systems was presented along with a method for designing PID control. The design procedure employs the modified Nichols diagram and its parameter specifications. The stability margins of the control system are specified directly in the diagram. Further, the numerical examples showed that the time responses can be stabilized for the required performance.

REFERENCES

G. S. Brown and D. P. Campbell. *Principles of Servomechanisms*, J. Wiley & Sons, 1948.

R. E. Curry. *Estimation and Control with Quantized Measurements*, Cambridge, MIT Press, 1970.

A. Datta, M.T. Ho and S.P. Bhattacharyya. *Structure and Synthesis of PID Controllers*, Springer-Verlag, 2000.

D. F. Delchamps. Stabilizing a Linear System with Quantized State Feedback. *IEEE Trans. on Automatic Control*, volume 35, pages 916–924, 1990.

C. A. Desoer and M. Vidyasagar. *Feedback System: Input-Output Properties*, Academic Press, 1975.

N. Elia and S. K. Mitter. Stabilization of Linear System with Limited Information. *IEEE Trans. on Automatic Control*, volume 46, pages 1384–1400, 2001.

M. Fu. Robust Stabilization of Linear Uncertain Systems via Quantized Feedback. *Proc. of the IEEE Int. Conf. on Decision and Control*, TuA06-5, 2003.

C. J. Harris and M. E. Valenca. *The Stability of Input-Output Dynamical Systems*, Academic Press, 1983.

R. E. Kalman. Nonlinear Aspects of Sampled-Data Control Systems. *Proc. of the Symposium on Nonlinear Circuit Analysis*, volume VI, pages 273–313, 1956.

Y. Okuyama *et al.*. Robust Stability Analysis for Nonlinear Sampled-Data Control Systems and the Aizerman Conjecture. *Proc. of the IEEE Int. Conf. on Decision and Control*, pages 849-852, 1998.

Y. Okuyama *et al.*. Robust Stability Evaluation for Sampled-Data Control Systems with a Sector Nonlinearity in a Gain-Phase Plane. *Int. J. of Robust and Nonlinear Control*, volume 9, No. 1, pages 15-32, 1999.

Y. Okuyama *et al.*. Robust Stability Analysis for Non-Linear Sampled-Data Control Systems in a Frequency Domain. *European Journal of Control*, volume 8, No. 2, pages 99–108, 2002.

Y. Okuyama *et al.*. Amplitude Dependent Analysis and Stabilization for Nonlinear Sampled-Data Control Systems. *Proc. of the 15th IFAC World Congress*, T-Tu-M08, 2002.

Y. Okuyama. Robust Stability Analysis for Discretized Nonlinear Control Systems in a Global Sense. *Proc. of the 2006 American Control Conference*, Minneapolis, USA, pages 2321–2326, 2006.

F. Takemori and Y. Okuyama. Discrete-Time Model Reference Feedback and PID Control for Interval Plants. *Digital Control 2000:Past, Present and Future of PID Control*, Pergamon Press, pages 260–265, 2000.

J. C. Willems. *The Analysis of Feedback Systems*, Cambridge, MIT Press, 1971.